ADVANCES IN ATMOSPHERIC SCIENCES, VOL. 39, OCTOBER 2022, 1777–1786

• Notes & Letters •

Importance of Air-Sea Coupling in Simulating Tropical Cyclone Intensity at Landfall

Charlie C. F. LOK[1], Johnny C. L. CHAN[*1], and Ralf TOUMI[*2]

[1]*School of Energy and Environment, City University of Hong Kong, Hong Kong, China*
[2]*Department of Physics, Imperial College, London SW7 2AZ, UK*

(Received 18 August 2021; revised 14 February 2022; accepted 9 March 2022)

ABSTRACT

An atmosphere-only model system for making seasonal prediction and projecting future intensities of landfalling tropical cyclones (TCs) along the South China coast is upgraded by including ocean and wave models. A total of 642 TCs have been re-simulated using the new system to produce a climatology of TC intensity in the South China Sea. Detailed comparisons of the simulations from the atmosphere-only and the fully coupled systems reveal that the inclusion of the additional ocean and wave models enable differential sea surface temperature responses to various TC characteristics such as translational speed and size. In particular, interaction with the ocean does not necessarily imply a weakening of the TC, with the coastal bathymetry possibly playing a role in causing a near-shore intensification of the TC. These results suggest that to simulate the evolution of TC structure more accurately, it is essential to use an air-sea coupled model instead of an atmosphere-only model.

Key words: tropical cyclone intensity, tropical cyclone landfall, seasonal prediction, air-sea coupling

Citation: Lok, C. C. F., J. C. L. Chan, and R. Toumi, 2022: Importance of air-sea coupling in simulating tropical cyclone intensity at landfall. *Adv. Atmos. Sci.*, **39**(10), 1777−1786, https://doi.org/10.1007/s00376-022-1326-9.

Article Highlights:

- Ocean has differential responses to the translational speed and size of tropical cyclones.
- Fast-moving and small tropical cyclones may intensify over a shallow continental shelf due to warmer ocean.
- Air-sea coupling is essential to accurate simulate tropical cyclone landfall intensities.

1. Introduction

Tropical cyclones (TCs) form and intensify over a large area of warm ocean water and can cause great damage to the coastal region when they make landfall. It is widely accepted that interactions between the ocean and the lower atmosphere play a crucial role in the evolution of TCs (Emanuel, 1986; Cione and Uhlhorn, 2003). A TC acquires its energy primarily from the underlying warm water via latent heat flux and spins up its circulation (Riehl, 1950). As the TC intensifies, its circulation induces subsurface ocean mixing and creates a cool pool of water, which in turn limits the energy supply and ultimately TC intensity (Schade and Emanuel, 1999; Chan et al., 2001; Vincent et al., 2012). Given its fundamental role in TC evolution, extensive research has been conducted to understand the air-sea interaction of TCs.

In order to closely examine the effects of air-sea interaction on TCs, numerical weather prediction models are often utilized. With a coupled air-sea model, Schade and Emanuel (1999) found that sea surface temperature (SST) cooling induced by a TC circulation substantially weakens the TC, and that the effect is most significant for slow-moving TCs or over thin oceanic mixed layers. A number of numerical and observational studies (e.g. Wada et al., 2014; Zarzycki, 2016; Zhao and Chan, 2017; Lengaigne et al., 2019) have further examined the impact of negative feedback of SST cooling on TC intensity and emphasized the necessity of atmosphere-ocean coupling. In addition to weakening, Wu et al. (2005) also identified a small southward drift in TC track due to the induced asymmetrical SST structure. However, little attention to this effect has been given since then.

If ocean coupling solely provides negative feedback on TC intensity, it might not be economical to run a three-dimensional coupled model. Alternatively, Liu et al. (2019) proposed a parameterization scheme to account for the effects of TC-induced mixing and cooling when using an atmosphere-only model. Recently studies have shown that not

* Corresponding authors: Johnny C. L. CHAN, Ralf TOUMI
Emails: Johnny.Chan@cityu.edu.hk, r.toumi@imperial.ac.uk

only subsurface ocean processes, but ocean waves can also affect TC intensity. Liu et al. (2011) performed idealized experiments using a coupled atmosphere-wave-ocean model to quantify the effects on TC intensity of various air-sea processes inside mature TCs. They also found that the ocean effects such as SST cooling tend to weaken TCs but influences of waves on TCs are more complicated. High waves induced by strong winds may on the one hand increase surface roughness and friction and subsequently weaken TCs, while the induced sea spray tends to increase heat and moisture fluxes and strengthen TCs (Andreas and Emanuel, 2001; Garg et al., 2018). Bruneau et al. (2018) showed that wave white-capping leads to substantial ocean cooling as TCs approach the coastal area.

In 2017, Typhoon Hato made landfall near Macau, causing tremendous damage and at least 25 fatalities in the region (Hong Kong Observatory, 2019). This TC had undergone rapid intensification just prior to landfall. Several studies have examined its physical mechanism. Zhang et al. (2019) identified the presence of barotropic eddy kinetic energy and large latent heat flux near the coastal region. The substantial amount of latent heat release during the passage of Hato (2017) was further analyzed by Pun et al. (2019), who reported that the continental shelf extending from South China, which is about 200 km away from the coast and less than 200 m depth, can account for the well-mixed warm water and thus the intensification of Typhoon Hato (2017). While the importance of the coastal ocean needs to be addressed, it remains unknown as to where the warm water comes from, and why not every TC will undergo such intensification. Lok et al. (2021) suggested that small TCs can potentially induce SST warming over the continental shelf and subsequent intensification prior to landfall.

It is clear from this brief review that the contribution of air-sea interaction in modifying TC characteristics is much more than a simple weakening of the TC. It is therefore necessary to include coupling of full-physics ocean and wave models with the atmosphere model in order to represent the various air-sea interaction processes under TC conditions.

Lok and Chan (2018a, hereafter LC) developed an atmosphere-only model system using a regional climate model to produce seasonal simulations with an 8-member ensemble of the large-scale environment of the western North Pacific and a mesoscale model to obtain the intensity at landfall of every TC produced by the regional model. During the 21-year simulation period between 1990 and 2010, the model produced a total of 642 TCs making landfall in South China. To investigate the influence of air-sea interaction on TC landfall intensity, we upgraded the model system by coupling an ocean model and a wave model to the mesoscale model, and re-simulated all the 642 TCs identified from the regional climate model outputs of LC.

This paper is organized as follows. Section 2 describes model design and data used. Section 3 compares the performance of the new air-sea coupled model system against the results of LC as well as a best-track dataset. Section 4 further examines the effects of ocean coupling on TC intensity. Finally, a summary is presented in section 5.

2. The new model system and data

2.1. *The COAWST modeling system*

The Coupled Ocean-Atmosphere-Wave-Sediment Transport modeling system version 3.2 revision 1192 (Warner et al., 2010, hereafter COAWST) is chosen as the air-sea coupled model to replace the mesoscale model used in LC. The COAWST model consists of three components: the Weather Research and Forecasting Model version 3.7.1 (Skamarock et al., 2008, hereafter WRF), the Regional Ocean Modeling System revision 838 (Shchepetkin and McWilliams, 2005, hereafter ROMS) and the Simulating WAves Nearshore model version 41.01AB (Booij et al., 1999, hereafter SWAN). The three models are connected by the Model Coupling Toolkit version 2.6.0 (Larson et al., 2005) to exchange information.

The WRF model is basically the same as that in LC, except its configurations are slightly adjusted for the coupling purposes. WRF solves the compressible, non-hydrostatic Euler equations of the atmosphere, with the following physical packages applied for subgrid processes: the WRF Single Movement class 6 scheme (Hong and Lim, 2006) for microphysics, the Yonsei University scheme (Hong et al., 2006) for the planetary boundary layer, Tiedtke (1989) scheme for cumulus convection in the outer domain, the Rapid Radiative Transfer Model (Iacono et al., 2008) for the radiative processes and the revised MM5 similarity scheme (Jiménez et al., 2012) for the surface layer. The WRF model has two stationary domains covering East Asia and northern South China Sea respectively (brown and red boxes in Fig. 1). The horizontal resolution of the outer (inner) domain is 18 km (6 km), with dynamic time step of 30 seconds (10 seconds). There are 37 vertical levels from the surface up to 20 hPa.

ROMS is a free-surface, bathymetry-following model, solving the Reynolds-averaged Navier-Stokes equations under the hydrostatic and incompressible assumptions for

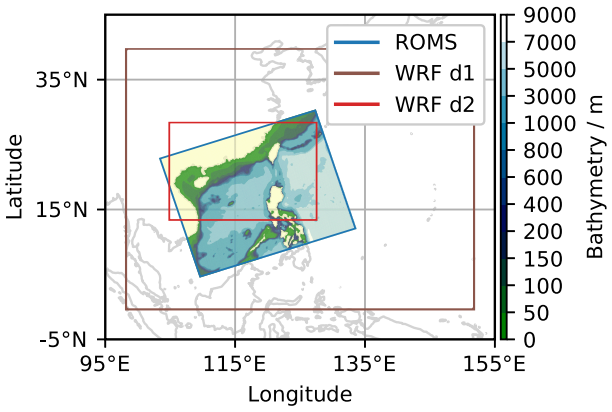

Fig. 1. Domain configurations of ROMS (blue), WRF outer (brown) and inner (red) grids. Colour shading represents the bathymetry (m) as seen by the ROMS model.

the ocean. The model has a single domain of 6 km horizontal resolution, covering the north South China Sea (blue box in Fig. 1). There are 21 sigma levels with higher resolution above 200 m depth.

The third generation SWAN model solves the wave action balance equation, including physical processes of wind-growth, white-capping, wave breaking, bottom friction and nonlinear wave-wave interactions. The model runs in a non-stationary mode with a time step of 2 minutes and has a spectral grid of 36 directions (10° resolution) and 25 frequencies. Its domain is the same as that of ROMS.

The different components of the coupled model system exchange information through the Model Coupling Toolkit. WRF obtains sea surface temperatures from ROMS, and in return provides states of the atmosphere at the boundary and heat fluxes back to ROMS. WRF also feeds the surface winds to SWAN and receives states of the sea-wave to modify friction velocity. Ocean currents from ROMS and wave energy dissipation from SWAN are shared between the two models.

2.2. *Data*

Since no modification is made to the regional climate model (the ICTP Regional Climate Model version 3 "RegCM", Pal et al., 2007) component of the LC model system, its outputs serve as the initial and boundary conditions of the atmospheric model for the 642 TCs identified, or exactly the same procedure as for the mesoscale model in LC.

The NCEP Climate Forecast System reanalysis data (CFSR, Saha et al., 2010) were used as the underlying SST in LC, and so the same dataset is used for the initial and boundary conditions of the ocean component of the new system. For the wave model, it is assumed that no wave exists before the model starts due to lack of data.

The COAWST model starts at the same time as the WRF model in LC for each TC, which is 60 hours prior to its landfall in RegCM. The results produced in this study are compared with (a) the results from LC, referred as the "WRF-only" model, and (b) the Joint Typhoon Warning Center (JTWC) Best Track dataset (Chu et al., 2002). Because the new model has a finer horizontal resolution (6 km) than that in LC, the wind fields from both model systems are interpolated to the same 9 km horizontal grid to determine TC intensity for evaluation.

3. Evaluation of the new model system

Among the 642 RegCM TCs, both model systems produce very similar intensities (Fig. 2a). The average peak intensity from the new system is 81.2 kt (1 kt = 1.852 km h^{-1}), which is just 0.8 kt higher (significant at the 95% confidence level) than from the old system. Overall, 53.7% of the TCs show the difference in the peak maximum sustained wind speed between the two models to be <5 kt (Fig. 2b). For the TC intensity at landfall, the mean difference is also very similar to that of peak intensity (Fig. 2c).

While differences in intensity between the two models

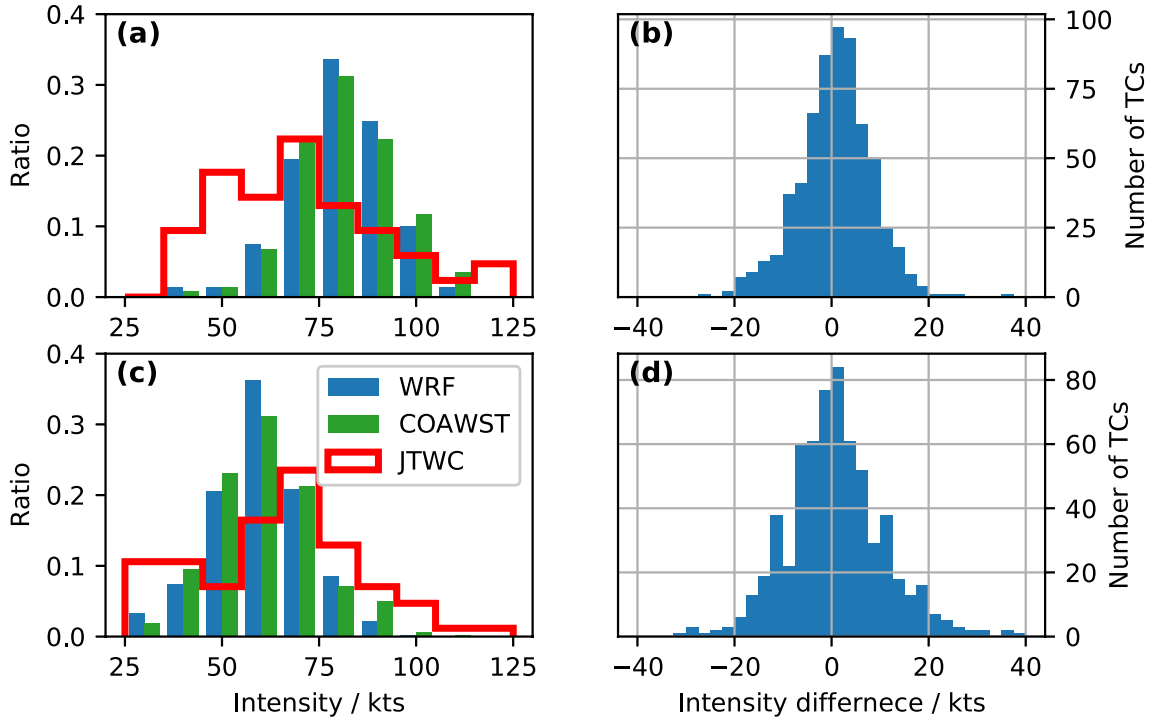

Fig. 2. Normalized distributions of (a) the peak TC intensity during the 60 hours prior to landfall in South China and (c) the TC intensity at landfall from the JTWC Best Track dataset (red outline), the WRF-only (blue) and the COAWST (green) models. Distribution of the differences in (b) TC peak intensity and (d) the TC intensity at landfall between the COAWST and WRF-only models. Positive value represents a stronger TC simulated by COAWST.

are small, the climatology produced by the new model system is slightly better than the old model. The normalized intensity distributions of the coupled model share 62.7% (at peak) and 72.6% (at landfall) common areas with those of the Best Track dataset, while the old system produced 3% less in both cases.

Liu and Chan (2017) proposed and utilized an annual power dissipation index (APDI), which is the sum of the cube of the maximum sustained wind speeds at the time of TC landfall in a region throughout one year, to analyze seasonal variability of TC landfall intensity. Here, APDI is also used to measure the performances of the two systems. The observed average APDI is 12.0×10^5 kt^3, while the coupled and the WRF-only models give values of 9.8×10^5 kt^3 and 9.3×10^5 kt^3 respectively. The root mean square error for the coupled model is 9.3×10^5 kt^3, which is 0.3×10^5 kt^3 smaller than the WRF model.

The ensemble spread of the new model system has also been improved slightly. Rank histogram (Anderson, 1996), which ranks the observation among the ensemble members from the smallest to the largest, is used to further assess the ensemble component. While both models can capture the observed APDI within their ensemble spreads in general (ranking 2–8 in Fig. 3), the COAWST model has 3 less outliners than the WRF model (highest rank in Fig. 3).

The above comparisons suggest that with the air-sea-wave coupling the model system has a slightly better skill in simulating TC intensity climatology. In the next section, differences of individual TCs and the physical mechanisms will be further analyzed.

4. Impact of air-sea interaction on TC intensity

Since the atmospheric model acquires ocean information primarily via SST, the overall effect of ocean coupling on SST over the South China Sea is examined. Two days before TCs made landfall, there is 0.2°C cooling of SST to the west of the Philippines (Fig. 4a), and in the next 24 hours the cooling area moves towards the South China coast because most TCs track northwestward, with the magnitude of cooling reaching 0.4°C (Fig. 4b). Such SST cooling is consistent with previous studies (e.g. Wada et al., 2014; Zarzycki, 2016; Zhao and Chan, 2017; Lengaigne et al., 2019). Apart from the TC-induced cooling, ocean warming of 0.2°C to 0.4°C is also observed near the coastal region two days before landfall, and near Hainan Island and Taiwan Strait during the final 24 hours. As these parts of the sea water are further away from the TC and rather shallow (< 200 m depth, see Fig. 1), the incoming solar energy can therefore effectively warm up the ocean as reported in Lok et al. (2021).

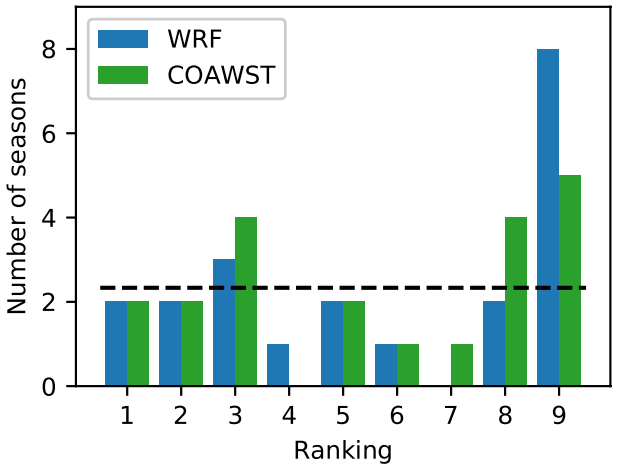

Fig. 3. Rank histograms of the APDI in South China of the WRF only (blue) and the COAWST (green) models. Dashed lines represent an idealized perfect ensemble model.

To further diagnose the impact of ocean coupling on the intensity simulation, TCs with at least 15 kt difference in intensity at landfall between the two models are divided into two groups: the "weaker" (COAWST TCs weaker; 4.5% of TCs) and the "stronger" (COAWST TCs more intense; 8.0% of TCs). For the "weaker" TCs, while the overall SST change due to air-sea coupling has similar patterns as for all TCs, the differences are more negative, with the maximum cooling reaching 0.8°C in the central South China Sea in the final 24 hours before TC making landfall (Figs. 4c and 4d). In contrast, for the "stronger" group, the COAWST-simulated SST is not even cooled between 48 and 24 hours ahead of landfall (Fig. 4e), and the cooling effect on the last day is much smaller (0.2°C, Fig. 4f). Apart from the SST difference, the "stronger" TCs have larger southwestward drift from the WRF-only TCs than the "weaker" group (Fig. 5), and consequently these TCs move even closer to the warm pool of water (red areas in Fig. 4e). As SST has a crucial role in TC intensity change (Emanuel, 1999; Balaguru et al., 2015), having warmer SST as well as tracking closer to the warm pool appear to be the main reasons of the difference in TC landfall intensities.

It is also important to understand how the TC itself may induce changes in the underlying ocean. Slow-moving TCs tend to generate stronger ocean mixing and negative feedback of SST on TC intensity (Mei et al., 2012; Zhao and Chan, 2017). Therefore, the effect of translational speed is first examined. Significant differences in TC translational speed are found between these two groups (Fig. 6). The "weaker" group has an average speed of 10.3 kt, which is 2.1 kt slower (significant at the 95% confidence level) than that in the "stronger" group.

Lok et al. (2021) reported that smaller TCs may self-induce intensification as they approach the coast. While there is no direct relationship between the TC size and how much stronger the TC can be with the ocean coupling, it appears that smaller TCs are indeed able to achieve greater intensity increase than the larger TCs (Fig. 7). Our results suggest that including air-sea coupling can produce more realistic TC intensity simulation.

To illustrate how the translational speed and the size of a TC may combine to affect the simulated SST, four example TCs are selected for demonstration: a fast-moving small TC

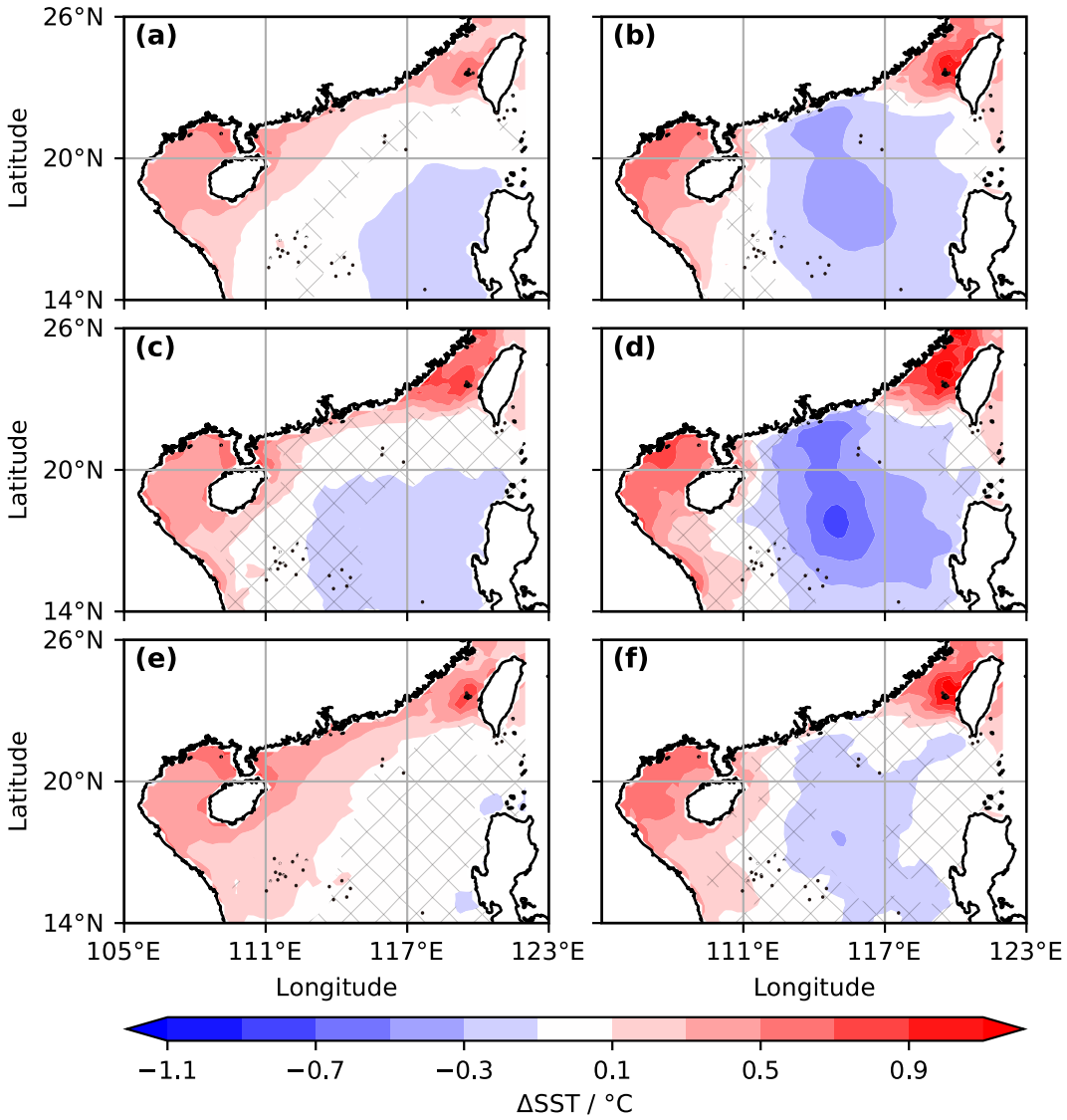

Fig. 4. Differences in daily mean SST (°C) between COAWST and WRF-only (a, c, e) two days and (b, d, f) one day prior to landfall for (a, b) all TCs, (c, d) the weaker and (e, f) the stronger groups. Positive values represent increases in the simulated SST. Differences not significant at 95% confidence level are crossed out.

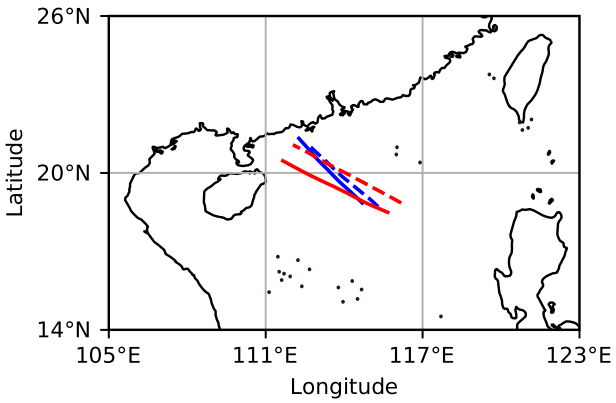

Fig. 5. Average TC tracks of the stronger group (red) and the weaker group (blue) during the 24-hour period before making landfall. Solid (dash) lines are produced by the coupled (WRF-only) model.

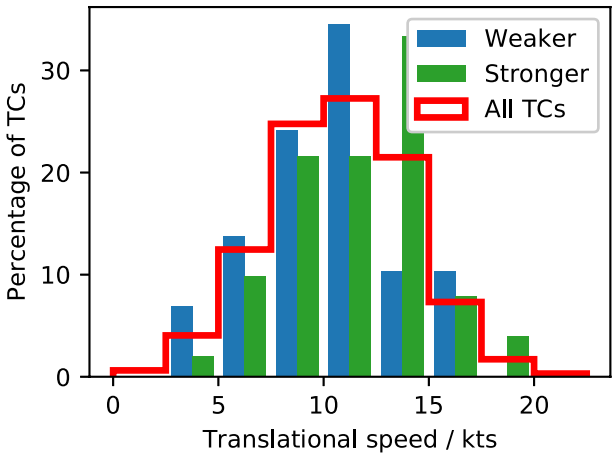

Fig. 6. Normalized distributions of the mean TC translational speed in the 24-hour period prior to landfall for all TCs (red outline), the weaker (blue) and the stronger (green) groups from COAWST.

"FAST-SMALL", a fast-moving large TC "FAST-LARGE", a slow-moving small TC "SLOW-SMALL", a slow-moving large TC "SLOW-LARGE". The "FAST-SMALL" TC travels across the South China Sea at an average speed of 12.6 kt (see the tracks in Fig. 8) and has a cloud cover with a 200-km radius (Fig. 9a). It experiences warmer SST in the COAWST model than in the WRF-only model throughout its passage over the South China Sea (Figs. 8b and d), especially near the South China coast where the SST increases by 0.6°C to 1.0°C ahead of the TC (Fig. 8a). Consequently, it makes landfall with maximum sustained wind speeds of 87.5 knots, 24 knots stronger than WRF-only and resembling Typhoon Hato (2017; Lok et al., 2021).

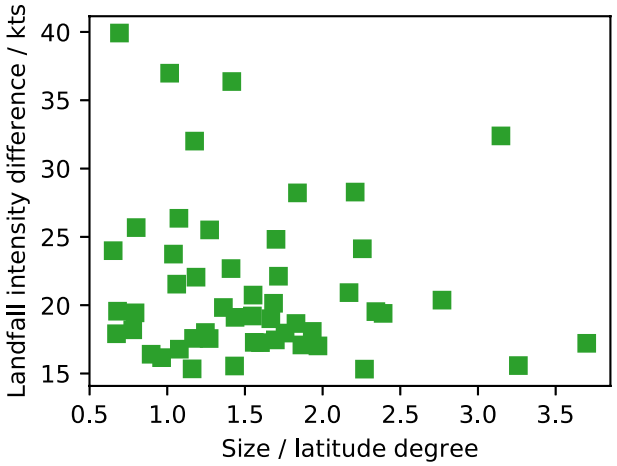

Fig. 7. Increase in TC landfall intensity due to ocean coupling as a function of TC size. TC size is defined as the mean radius of cloud cover exceeding 85%.

The "FAST-LARGE" TC moves even faster at 14.5 kt (see the tracks in Fig. 10), but its increase in landfall intensity due to ocean coupling is only 6 kt. The "FAST-LARGE" TC has a 500-km radius cloud cover (Fig. 9c), blocking sunlight reaching the ocean especially over the continental shelf, and hence no heating of the water in most parts of South China Sea (Figs. 10a and c). As reported in Lok et al. (2021), the effect of ocean-coupling becomes smaller for large TCs.

On the other hand, the "SLOW-SMALL" TC is 8 kt weaker at landfall in COAWST than that in the WRF-only model, and no near-shore SST-warming is simulated (Figs. 11a and c). Instead, it experiences similar or even colder sea water than the WRF-only model prior to landfall (Figs. 11b and d). The "SLOW-SMALL" TC moves at a

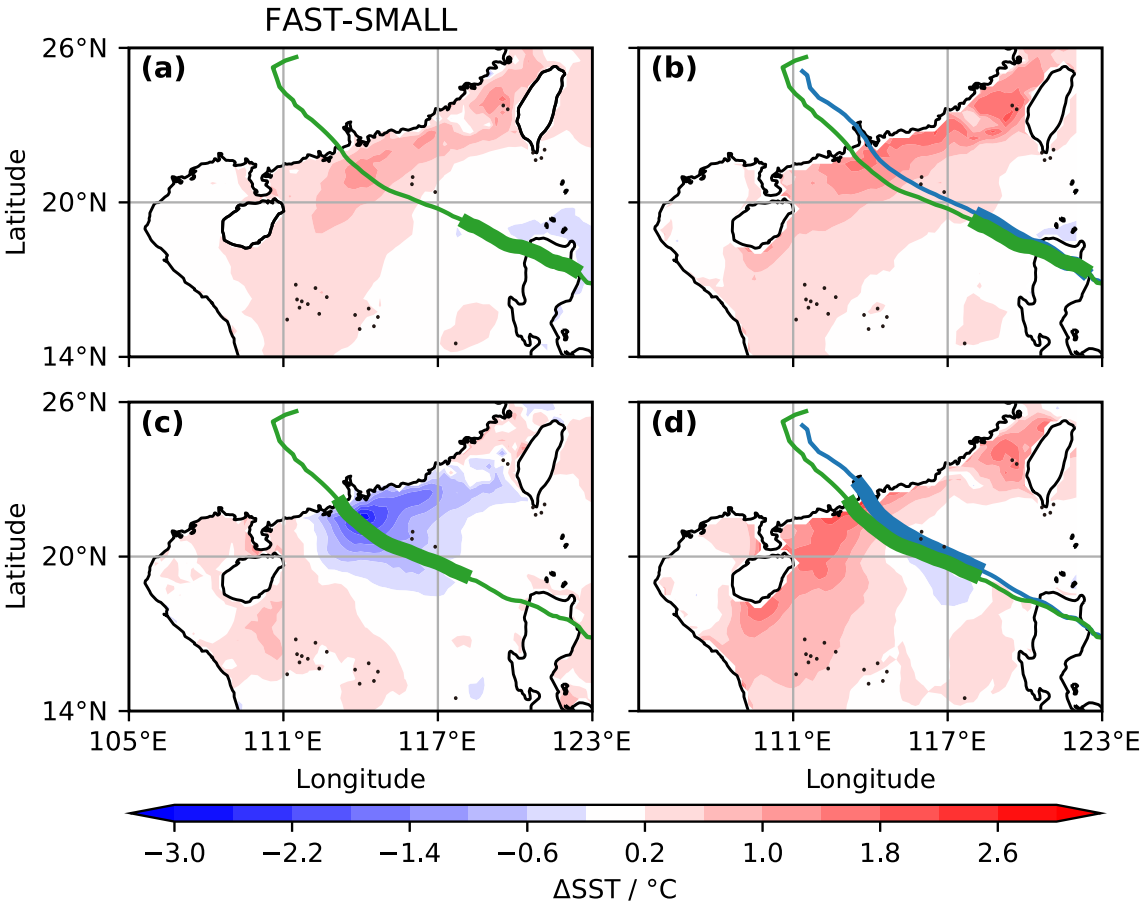

Fig. 8. (a, c) 24-hour SST changes simulated by COAWST and (b, d) differences in daily mean SST between COAWST and WRF-only (a, b) two days and (c, d) one day prior to landfall for the example TC "FAST-SMALL". TC tracks produced by WRF-only and COAWST are plotted in blue and green respectively, with squares showing the corresponding time period.

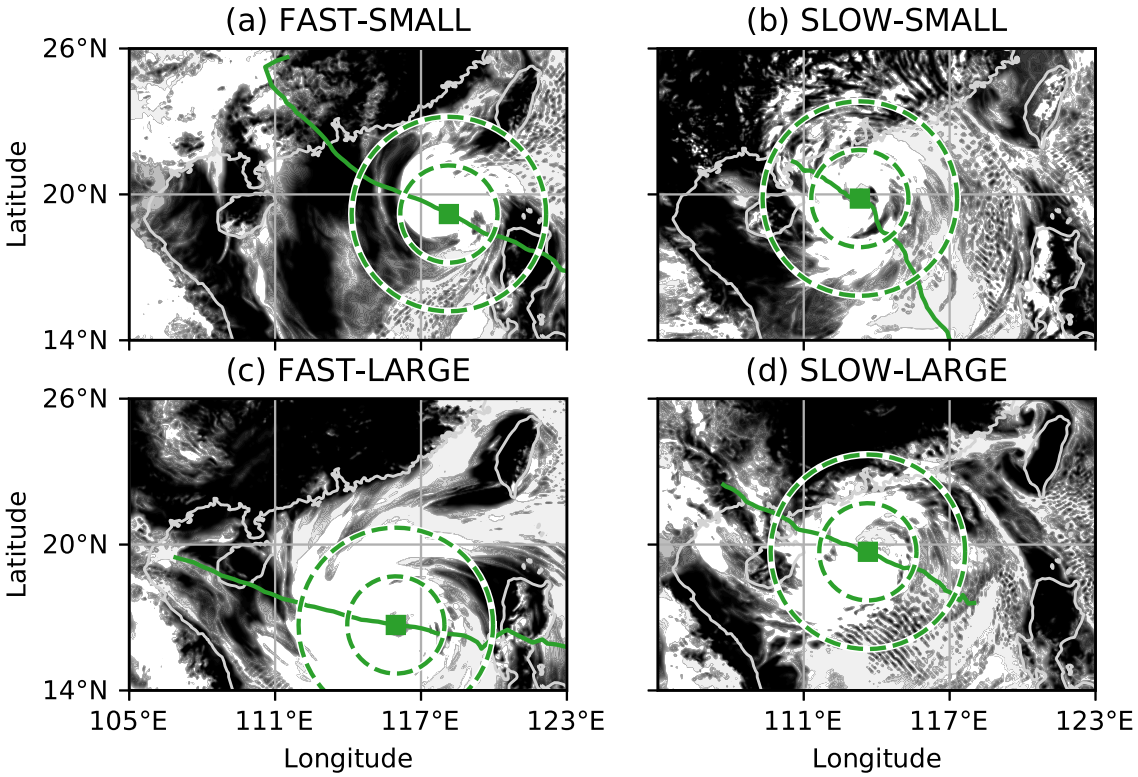

Fig. 9. COAWST simulated cloud cover at 24 hours prior to landfall for the example TC (a) "FAST-SMALL", (b) "SLOW-SMALL", (c) "FAST-LARGE" and (d) "SLOW-LARGE". Green lines are the TC track, with squares indicating their positions. 200 and 400 km away from the TCs are drawn in green dashed lines.

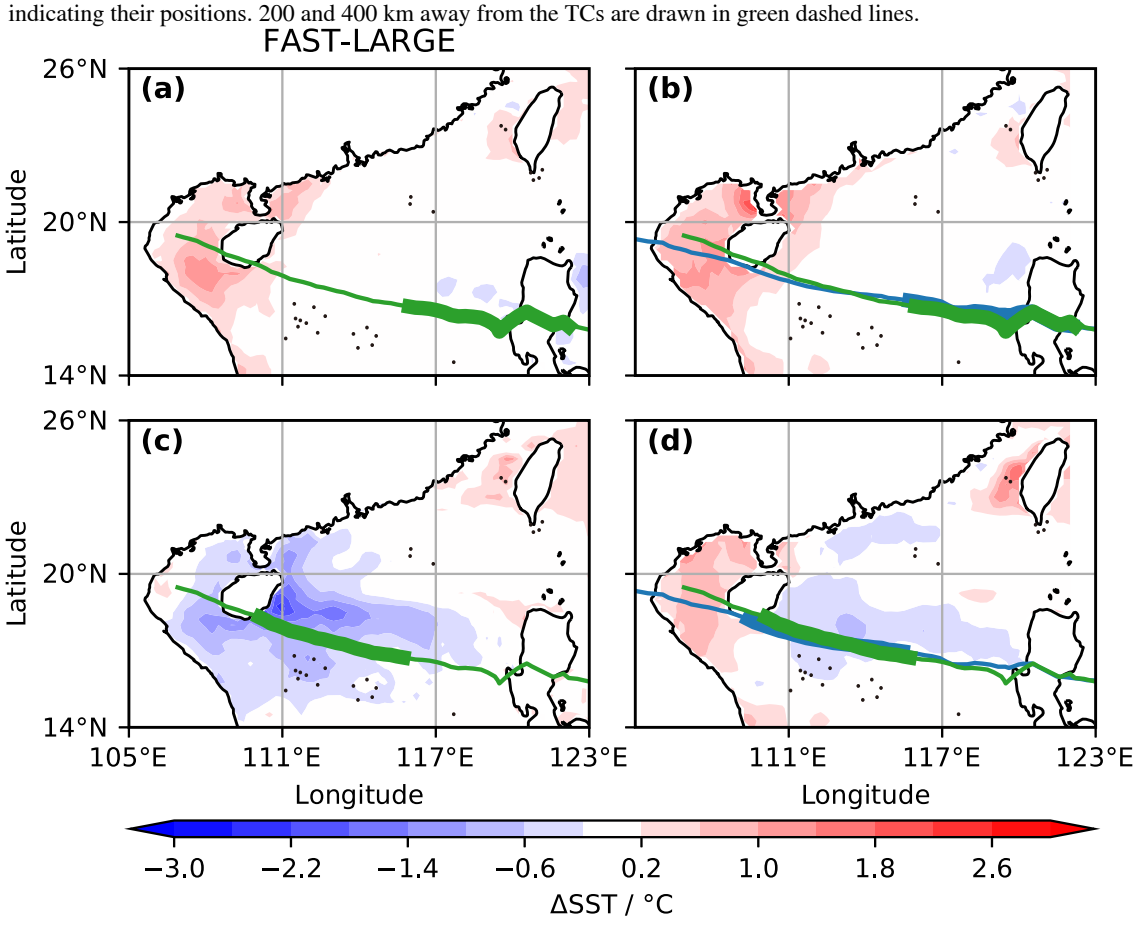

Fig. 10. As Fig. 8, except for the example TC "FAST-LARGE".

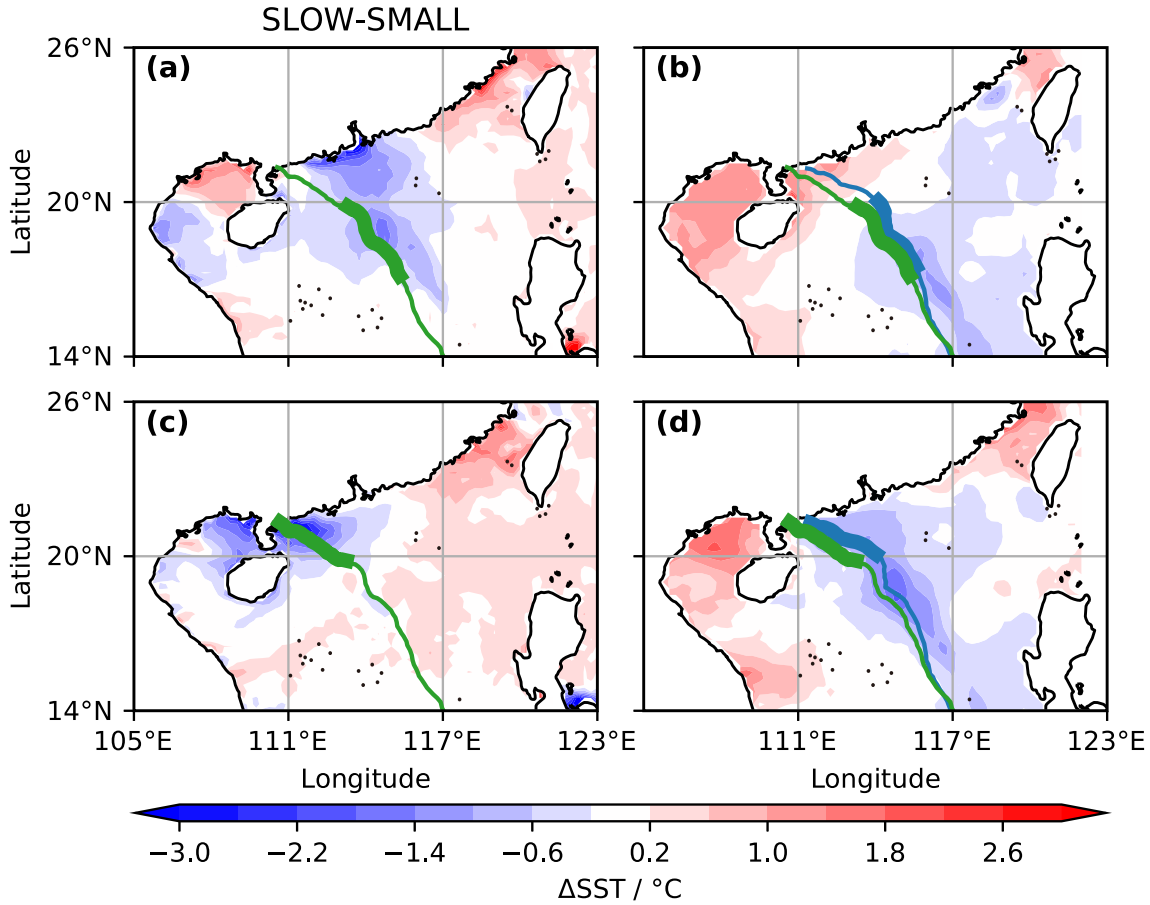

Fig. 11. As Fig. 8, except for the example TC "SLOW-SMALL".

mean speed of 7.2 kt, triggering stronger SST cooling and subsequent negative feedback on TC intensity (Mei et al., 2012; Vincent et al., 2012). Furthermore, if a slow-moving TC also has an extensive cloud cover (the "SLOW-LARGE" TC, Fig. 9d), the combined effect of ocean upwelling and sunlight blocking will make the COAWST TC much weaker (16 kt for the "SLOW-LARGE" TC).

These results therefore demonstrate that it is essential to include air-sea coupling to simulate TC evolution, as the interactions between TC and the underlying ocean can affect the resulting intensity, especially before landfall over a shallow continental shelf.

5. Summary

To better understand and predict TC intensity change, we have upgraded the model system developed by LC by replacing the atmosphere-only mesoscale model with an air-sea-wave fully-coupled model. While the re-simulated climatology of the 642 TCs is very similar to that of the previous model, the new system produces a slightly better climatology of TC peak intensity as well as the intensity at the time of making landfall in South China.

More importantly, the fully-coupled system highlights the differential SST responses to individual TCs. In agreement with previous studies, the underlying ocean is cooled more if TCs move slower (e.g. Mei et al., 2012; Zhao and Chan, 2017), and TCs are less likely to be stronger if they have extensive cloud covers as reported in the case studies of Lok et al. (2021). Such differential SST responses can then lead to large differences in landfall intensity. These results demonstrate that the underlying ocean reacts differently to each TC. Using a fully-coupled air-wave-sea model is therefore necessary to predict TC intensity change, especially near landfall.

Given the better skills of the new model system, it can be used either in the prediction of TC intensity at landfall, or in projecting future variations, as has been done by Lok and Chan (2018b) using an atmosphere-only model. Results from these studies will be reported in the near future.

Acknowledgements. This research is supported by Hong Kong Research Grants Council Grant CityU E-CityU101/16. RT was supported by the Natural Environment Research Council/ UKRI (Grant No. NE/V017756/1).

Data Availability. The COAWST model is available at https://coawstmodel-trac.sourcerepo.com/coawstmodel_COAWST/, and its configurations are described in section 2. Initial and boundary conditions are taken from CFSR at https://www.ncei.noaa.gov/products/weather-climate-models/climate-forecast-system. JTWC best track can be downloaded from https://www.metoc.navy.mil/jtwc/

jtwc.html?best-tracks. SST and simulated TC tracks produced in this study and LC are available at http://doi.org/10.5281/zenodo.5048538.

REFERENCES

Anderson, J. L., 1996: A method for producing and evaluating probabilistic forecasts from ensemble model integrations. *J. Climate*, **9**(7), 1518–1530, https://doi.org/10.1175/1520-0442(1996)009<1518:AMFPAE>2.0.CO;2.

Andreas, E. L., and K. A. Emanuel, 2001: Effects of sea spray on tropical cyclone intensity. *J. Atmos. Sci.*, **58**(24), 3741–3751, https://doi.org/10.1175/1520-0469(2001)058<3741:EOSSOT>2.0.CO;2.

Balaguru, K., G. R. Foltz, L. R. Leung, E. D'Asaro, K. A. Emanuel, H. L. Liu, and S. E. Zedler, 2015: Dynamic potential intensity: An improved representation of the ocean's impact on tropical cyclones. *Geophys. Res. Lett.*, **42**(16), 6739–6746, https://doi.org/10.1002/2015GL064822.

Booij, N., R. C. Ris, and L. H. Holthuijsen, 1999: A third-generation wave model for coastal regions: 1. Model description and validation. *J. Geophys. Res.: Oceans*, **104**(C4), 7649–7666, https://doi.org/10.1029/98JC02622.

Bruneau, N., R. Toumi, and S. Wang, 2018: Impact of wave whitecapping on land falling tropical cyclones. *Scientific Reports*, **8**(1), 652, https://doi.org/10.1038/s41598-017-19012-3.

Chan, J. C. L., Y. H. Duan, and L. K. Shay, 2001: Tropical cyclone intensity change from a simple ocean-atmosphere coupled model. *J. Atmos. Sci.*, **58**(2), 154–172, https://doi.org/10.1175/1520-0469(2001)058<0154:TCICFA>2.0.CO;2.

Chu, J. H., C. R. Sampson, A. S. Levine, and E. Fukada, 2002: The joint typhoon warning center tropical cyclone best-tracks, 1945–2000. Report NRL/MR/7540-02-16.

Cione, J. J., and E. W. Uhlhorn, 2003: Sea surface temperature variability in hurricanes: Implications with respect to intensity change. *Mon. Wea. Rev.*, **131**(8), 1783–1796, https://doi.org/10.1175//2562.1.

Emanuel, K. A., 1986: An air-sea interaction theory for tropical cyclones. Part I: Steady-state maintenance. *J. Atmos. Sci.*, **43**(6), 585–605, https://doi.org/10.1175/1520-0469(1986)043<0585:AASITF>2.0.CO;2.

Emanuel, K. A., 1999: Thermodynamic control of hurricane intensity. *Nature*, **401**(6754), 665–669, https://doi.org/10.1038/44326.

Garg, N., E. Y. K. Ng, and S. Narasimalu, 2018: The effects of sea spray and atmosphere-wave coupling on air-sea exchange during a tropical cyclone. *Atmospheric Chemistry and Physics*, **18**(8), 6001–6021, https://doi.org/10.5194/acp-18-6001-2018.

Hong Kong Observatory, 2019: Tropical Cyclone in 2017. Hong Kong, China. https://www.hko.gov.hk/en/publica/tc/files/TC2017.pdf.

Hong, S.-Y., and J.-O. J. Lim, 2006: The WRF single-moment 6-class microphysics scheme (WSM6). *Journal of the Korean Meteorological Society*, **42**(2), 129–151.

Hong, S.-Y., Y. Noh, and J. Dudhia, 2006: A new vertical diffusion package with an explicit treatment of entrainment processes. *Mon. Wea. Rev.*, **134**(9), 2318–2341, https://doi.org/10.1175/MWR3199.1.

Iacono, M. J., J. S. Delamere, E. J. Mlawer, M. W. Shephard, S. A. Clough, and W. D. Collins, 2008: Radiative forcing by long-lived greenhouse gases: Calculations with the AER radiative transfer models. *J. Geophys. Res.*, **113**(D13), D13103, https://doi.org/10.1029/2008JD009944.

Jiménez, P. A., J. Dudhia, J. F. González-Rouco, J. Navarro, J. P. Montávez, and E. García-Bustamante, 2012: A revised scheme for the WRF surface layer formulation. *Mon. Wea. Rev.*, **140**(3), 898–918, https://doi.org/10.1175/MWR-D-11-00056.1.

Larson, J., R. Jacob, and E. Ong, 2005: The model coupling toolkit: A new Fortran90 toolkit for building multiphysics parallel coupled models. *The International Journal of High Performance Computing Applications*, **19**(3), 277–292, https://doi.org/10.1177/1094342005056115.

Lengaigne, M., and Coauthors, 2019: Influence of air-sea coupling on Indian Ocean tropical cyclones. *Climate Dyn.*, **52**(1), 577–598, https://doi.org/10.1007/s00382-018-4152-0.

Liu, B., H. Q. Liu, L. Xie, C. L. Guan, and D. L. Zhao, 2011: A coupled atmosphere-wave-ocean modeling system: Simulation of the intensity of an idealized tropical cyclone. *Mon. Wea. Rev.*, **139**(1), 132–152, https://doi.org/10.1175/2010MWR3396.1.

Liu, K. S., and J. C. L. Chan, 2017: Variations in the power dissipation index in the East Asia region. *Climate Dyn.*, **48**(5-6), 1963–1985, https://doi.org/10.1007/s00382-016-3185-5.

Liu, X., J. Wei, D.-L. Zhang, and W. Miller, 2019: Parameterizing sea surface temperature cooling induced by tropical cyclones: 1. Theory and an application to typhoon Matsa (2005). *J. Geophys. Res.: Oceans*, **124**(2), 1215–1231, https://doi.org/10.1029/2018JC014117.

Lok, C. C. F., and J. C. L. Chan, 2018a: Simulating seasonal tropical cyclone intensities at landfall along the South China coast. *Climate Dyn.*, **50**(7–8), 2661–2672, https://doi.org/10.1007/s00382-017-3762-2.

Lok, C. C. F., and J. C. L. Chan, 2018b: Changes of tropical cyclone landfalls in South China throughout the twenty-first century. *Climate Dyn.*, **51**(7–8), 2467–2483, https://doi.org/10.1007/s00382-017-4023-0.

Lok, C. C. F., and J. C. L. Chan, and R. Toumi, 2021: Tropical cyclones near landfall can induce their own intensification through feedbacks on radiative forcing. *Communications Earth and Environment*, **2**, 184, https://doi.org/10.1038/s43247-021-00259-8.

Mei, W., C. Pasquero, and F. Primeau, 2012: The effect of translation speed upon the intensity of tropical cyclones over the tropical ocean. *Geophys. Res. Lett.*, **39**(7), L07801, https://doi.org/10.1029/2011GL050765.

Pal, J. S., and Coauthors, 2007: Regional climate modeling for

the developing world: The ICTP RegCM3 and RegCNET. *Bull. Amer. Meteor. Soc.*, **88**(9), 1395–1410, https://doi.org/10.1175/BAMS-88-9-1395.

Pun, I.-F., and Coauthors, 2019: Rapid intensification of typhoon Hato (2017) over shallow water. *Sustainability*, **11**(13), 3709, https://doi.org/10.3390/su11133709.

Riehl, H., 1950: A model of hurricane formation. *J. Appl. Phys.*, **21**(9), 917–925, https://doi.org/10.1063/1.1699784.

Saha, S., and Coauthors, 2010: The NCEP climate forecast system reanalysis. *Bull. Amer. Meteor. Soc.*, **91**(8), 1015–1058, https://doi.org/10.1175/2010BAMS3001.1.

Schade, L. R., and K. A. Emanuel, 1999: The ocean's effect on the intensity of tropical cyclones: Results from a simple coupled atmosphere-ocean model. *J. Atmos. Sci.*, **56**(4), 642–651, https://doi.org/10.1175/1520-0469(1999)056<0642:TOSEOT>2.0.CO;2.

Shchepetkin, A. F., and J. C. McWilliams, 2005: The regional oceanic modeling system (ROMS): A split-explicit, free-surface, topography-following-coordinate oceanic model. *Ocean Modelling*, **9**(4), 347–404, https://doi.org/10.1016/j.ocemod.2004.08.002.

Skamarock, W. C., and Coauthors, 2008: A description of the advanced research WRF version 3. NCAR/TN-475+STR.

Tiedtke, M., 1989: A comprehensive mass flux scheme for cumulus parameterization in large-scale models. *Mon. Wea. Rev.*, **117**(8), 1779–1800, https://doi.org/10.1175/1520-0493(1989)117<1779:ACMFSF>2.0.CO;2.

Vincent, E. M., M. Lengaigne, J. Vialard, G. Madec, N. C. Jourdain, and S. Masson, 2012: Assessing the oceanic control on the amplitude of sea surface cooling induced by tropical cyclones. *J. Geophys. Res.: Oceans*, **117**(C5), C05023, https://doi.org/10.1029/2011JC007705.

Wada, A., T. Uehara, and S. Ishizaki, 2014: Typhoon-induced sea surface cooling during the 2011 and 2012 typhoon seasons: Observational evidence and numerical investigations of the sea surface cooling effect using typhoon simulations. *Progress in Earth and Planetary Science*, **1**(1), 11, https://doi.org/10.1186/2197-4284-1-11.

Warner, J. C., B. Armstrong, R. Y. He, and J. B. Zambon, 2010: Development of a coupled ocean-atmosphere-wave-sediment transport (COAWST) modeling system. *Ocean Modelling*, **35**(3), 230–244, https://doi.org/10.1016/j.ocemod.2010.07.010.

Wu, L. G., B. Wang, and S. A. Braun, 2005: Impacts of air-sea interaction on tropical cyclone track and intensity. *Mon. Wea. Rev.*, **133**(11), 3299–3314, https://doi.org/10.1175/MWR3030.1.

Zarzycki, C. M., 2016: Tropical cyclone intensity errors associated with lack of two-way ocean coupling in high-resolution global simulations. *J. Climate*, **29**(23), 8589–8610, https://doi.org/10.1175/JCLI-D-16-0273.1.

Zhang, R. W., J. L. Huangfu, and T. Hu, 2019: Dynamic mechanism for the evolution and rapid intensification of typhoon Hato (2017). *Atmospheric Science Letters*, **20**(8), e930, https://doi.org/10.1002/asl.930.

Zhao, X. H., and J. C. L. Chan, 2017: Changes in tropical cyclone intensity with translation speed and mixed-layer depth: Idealized WRF-ROMS coupled model simulations. *Quart. J. Roy. Meteor. Soc.*, **143**(702), 152–163, https://doi.org/10.1002/qj.2905.